



Communication

A 3D printable self-healing composite conductive polymer for sensitive temperature detection



Mengnan He, Yan Zhao, Yunqi Liu, Dacheng Wei*

State Key Laboratory of Molecular Engineering of Polymers, Department of Macromolecular Science, Fudan University, Shanghai 200433, China

ARTICLE INFO

Article history:

Received 24 March 2019

Received in revised form 16 April 2019

Accepted 3 June 2019

Available online 3 June 2019

Keywords:

Composite conductive polymer

Self-healing

3D printing

Temperature detection

Electronic device

ABSTRACT

Recent development of self-healing material has attracted tremendous attention, owing to its biomimetic ability to restore structure and functionality when encountering damages. Here, we develop a three-dimensional (3D) printable self-healing composite conductive polymer by mixing hydrogen-bond-based supramolecular polymer with low-cost carbon black. It has a room-temperature self-healing capability in both conductivity and mechanical property, while its shear-thinning behavior enables fabrication of a self-healable circuit by 3D printing technology. As an application, the circuit shows an excellent temperature-dependent behavior of the resistance, indicating its great potential for practical application in the artificial intelligence field.

© 2019 Chinese Chemical Society and Institute of Materia Medica, Chinese Academy of Medical Sciences. Published by Elsevier B.V. All rights reserved.

Three-dimensional (3D) printing is an additive manufacture technology, which creates complex structural or functional objects through adding materials layer-by-layer [1–5]. Extrusion printing is an extrusion-based 3D printing technique by depositing viscous material directly that rapidly solidifies upon extrusion [6]. Till now, 3D printing technology has become an increasing interest for scientists of electronics as it enables the manufacture of large-area, flexible electronics at low-cost [7–11]. For example, Leigh *et al.* demonstrated the carbon black/thermoplastic polymer composite for 3D-printed strain sensors [12]. Zhang *et al.* reported the reduced graphene oxide/poly(lactic acid) composite for flexible circuits [13]. However, the conductivity of these electronic devices cannot recover to their original state after undergoing deformation or fracture. To enhance the reliability and extend the lifetime in practical applications, it is vital to introduce self-healing property to these soft electronic devices that can repeatedly recover mechanical and electrical performance after damage under room temperature. Here, we develop a self-healing composite conductive polymer by combining the carbon black particles (CB) and hydrogen-bond-based self-healing polymer (HSP) through solution blending method. This CB/HSP composite has bulk electrical conductivity and self-healing property under ambient condition. The composite ink exhibits shear-thinning behavior, enabling fabrication of a self-healable electronic circuit by 3D printing. The circuit shows an excellent temperature-dependent behavior of the

resistance with a ratio up to ~90% when the temperature varies from 25 °C to 70 °C, higher than that of the carbon nanotube/HSP composite (30%) reported previously.

Before preparing CB/HSP composite, the HSP materials was synthesized by modified Leibler's method [14]. Briefly, 20.3 g of fatty acid (70 wt% triacids and 30 wt% diacids, Demand Chemical Co., Ltd. Shanghai) was reacted with 8 g of diethylenetriamine (Sigma-Aldrich) at 160 °C for 24 h under argon atmosphere with intensive magnetic stirring. Then, the product was dissolved in 100 mL chloroform by stirring and washed with 100 mL deionized water and 50 mL methanol, followed by removal of the residual chloroform by rotary evaporation. To prepare the CB/HSP composite, CB particles were dispersed in chloroform by ultrasonic for 1 h. Then, the HSP/CHCl₃ solution was slowly added into CB/CHCl₃ by stirring. The mixture was stirred overnight to ensure the uniformity of the composite. The solid composite was obtained by heating the mixture on the hot plate at 70 °C to remove the solvent. 3D printing ink was prepared by adding chloroform into the composite through stirring until the composite became viscous, and the added volume of chloroform was 12 mL when adding 1 g CB particles every time.

The morphology of CB and CB/HSP was characterized by using scanning electron microscope (SEM, Ultra 55). The Fourier transform infrared (FTIR) spectroscopy measurement was carried out on a Nicolet Nexus 6700 spectrometer. The healing process of the CB/HSP composite was characterized with an optical microscope (BH2, Olympus). All rheological measurements were obtained on a HAAKE MARS modular advanced rheometer using the 25 mm parallel-plate geometry. For 3D-printing, 3D Bio-Architects (work station,

* Corresponding author.

E-mail address: weidc@fudan.edu.cn (D. Wei).

Regenovo) was utilized to print various patterns and circuits. The electrical property was measured by using semiconductor analyzer (Keysight B1500A) and the probe station (Everbeing, PE-4). The temperature detection measurement was performed on a hot plate (SET, FYL201) and the temperature was changed every seven minutes to get stable current.

HSP is a supramolecular polymer with hydrogen-bonding network [14]. It is prepared by the condensation reaction of diethylene triamine with a mixture of fatty di-acid and tri-acids (Figs. S1 and S2 in Supporting information). The infrared spectra indicate that the hydrogen bonds are formed between N–H and C=O species (Fig. S3 in Supporting information). CB particles are dispersed in HSP polymer through solution blending method as illustrated in Fig. 1a. HSP supramolecular network provides the self-healing function via large number of hydrogen bonds, while the contact between CB particles provides the conductive channel. The CB particles are typical of grape-like morphology with the smooth surface after adding HSP polymer (Figs. 1b and c), implying that the CB particles are wrapped by HSP. Owing to the oxygen-containing functional group on the CB surface [15], the interface bonding force between CB and HSP is strong. Thus, it is indistinct to see the interface between CB and HSP, indicating the homodisperse of the CB particles in HSP. As we all known, the good dispersing and the strong interface bonding force are important to the conductivity of the composite. To evaluate the percolation threshold, the composites containing different weight fractions of CB were pressed into a square solid film of 10.0mm × 10.0mm × 0.4 mm (length × width × thickness) dimensions to measure the corresponding resistivity (Fig. 1d). The percolation threshold was measured about 3 wt%, in good agreement with the previous literature [16]. In this work, 15 wt% composite was used for the measurement and 3D printing applications.

The CB/HSP composite can be healed autonomously to the original state at room temperature within 5 h after making scratches on the surface (Figs. 2a and b). The healing time versus conductivity change is shown in Fig. 2c. After contacting two fractured halves together for 5 s, the current quickly increases. After 12 s, the current reaches a plateau and almost restores to the original value. Fig. 2d shows the resistance recovery against successive cut at the same location after healing for 5 h at room temperature. The resistance increases by < 2 times after the third

healing process. The electrical healing efficiency (η_E), which is calculated by the proportion of conductivity restored relative to the original conductivity [17], is up to 71% after first healing process and 54% after third healing process. This result indicates that most conduction channels are recovered after healing. As an application, a self-healing circuit based on the CB/HSP composite (Fig. 2e) was fabricated to connect a light-emitting diode (LED) lampion (3.0V). The electrical conductivity of the CB/HSP is determined by the proximity of the CB filler particles, the re-association of the hydrogen bonds within the HSP polymer and the resulting polymer flow enables re-establish physical contact between the CB filler particles (Fig. 2f). As a result, the LED was shining again after contacting the cut pieces together for 5 min under ambient condition.

The strain amplitude sweep test of the CB/HSP composite was performed as shown in Fig. 3a, showing that the critical strain of the G' (storage modulus) and G'' (loss modulus) (strains where both modulus experience a dramatic drop as the hydrogen-bond network fails) was 8%. With a value higher than 8%, the composite behaves like a liquid. In order to investigate the self-healing ability of CB/HSP, the continuous step strain experiment was performed as shown in Fig. 3b. G' and G'' changed as the strain altered between low (0.1%) and high (9%) oscillation excitations at room temperature. At first sequence, when the composite was under the small amplitude oscillatory shear (0.1%) for 10 min, the G' (870 MPa) was bigger than the G'' (460 MPa), indicating that the composite exhibited a solid-like property with hydrogen-bond network conserved. When the composite was subjected to a high amplitude oscillatory shear (9%), G' decreased to around 150 MPa lower than G'' (260 MPa), indicating that the hydrogen-bond network broke and the composite lost its solid-like property. Subsequently, when the strain reduced to 0.1% again, both G' and G'' recovered to the original state, which was attributed to the recovery of the hydrogen-bond network [18]. The healing efficiency of mechanical property (η_M) is calculated by [19]:

$$\eta_M = (G'_t / G'_0) \times 100$$

Where G'_t is the storage modulus of the composite at a defined time t and G'_0 is the storage modulus of the intact composite monitored at 0.1% strain. The η_M reaches to 89% after first healing process and remains 78% after the third healing process. For 3D

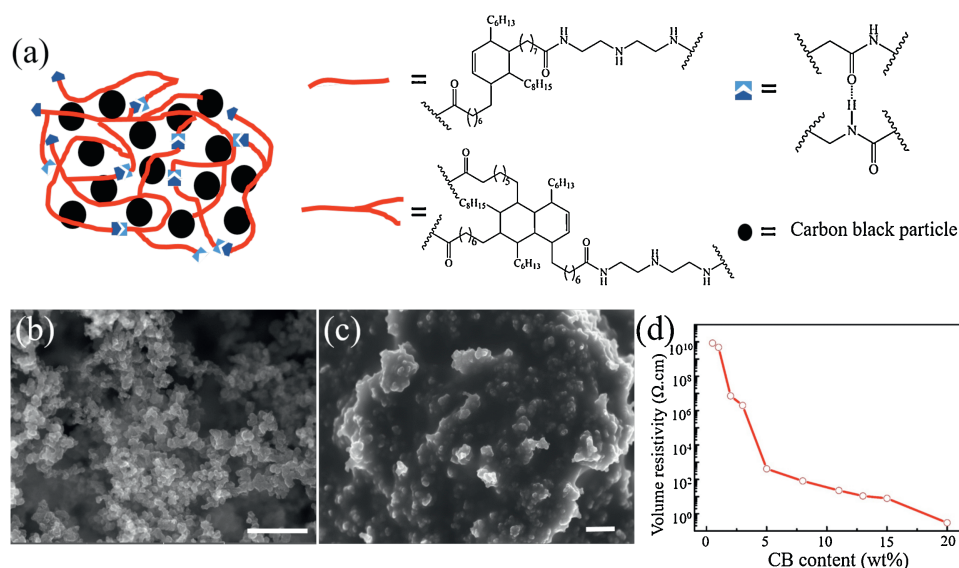


Fig. 1. (a) Schematic diagram of CB/HSP composite. Red lines represent the randomly branched HSP network, blue shapes represent hydrogen bonds between the polymer chains. (b, c) SEM images of CB and CB/HSP composite (15 wt%) respectively. The scale bars are 500 nm. (d) Volume resistivity of CB/HSP composite at different weight fractions of CB.

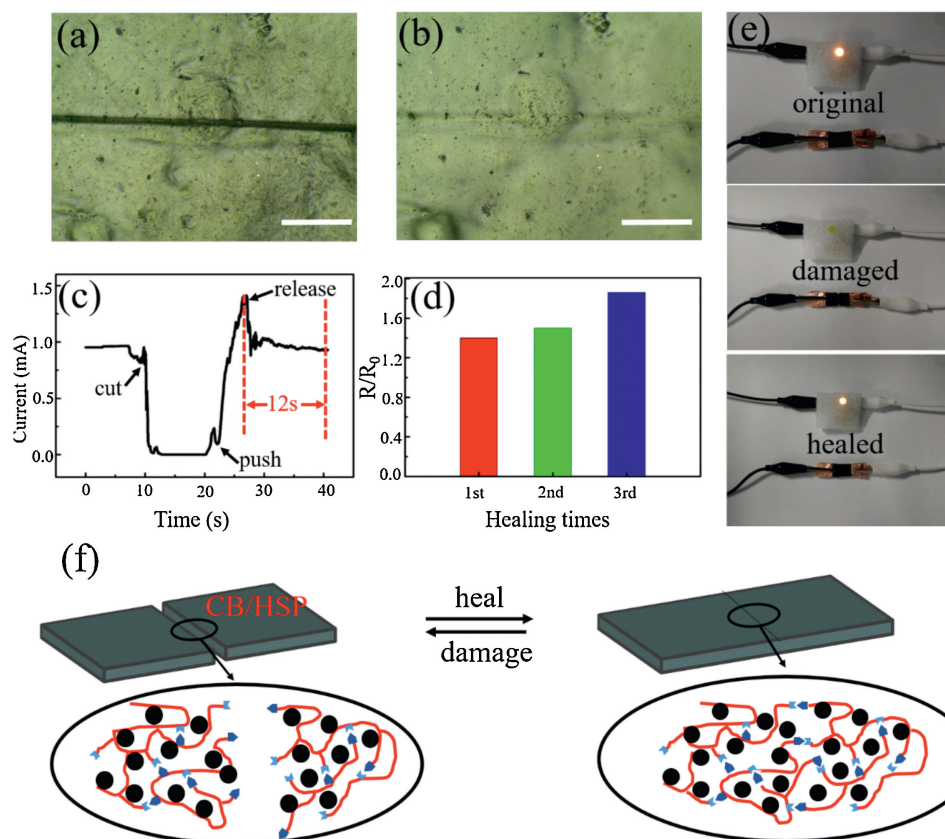


Fig. 2. (a, b) The optical microscopy images of damaged and complete healing composite (15 wt%), respectively. The scale bars are 200 μm. (c) Time evolution of the electrical healing process at 20 V voltages under room temperature. To heal the samples, the two fractured halves were pushed together by applying a gentle pressure for 5 s. (d) Repeated electrical healing for three times cuts at the same location. (e) The demonstration of the healing process for a conductive composite with a LED in series. (f) Schematic healing mechanism of the composite after cut.

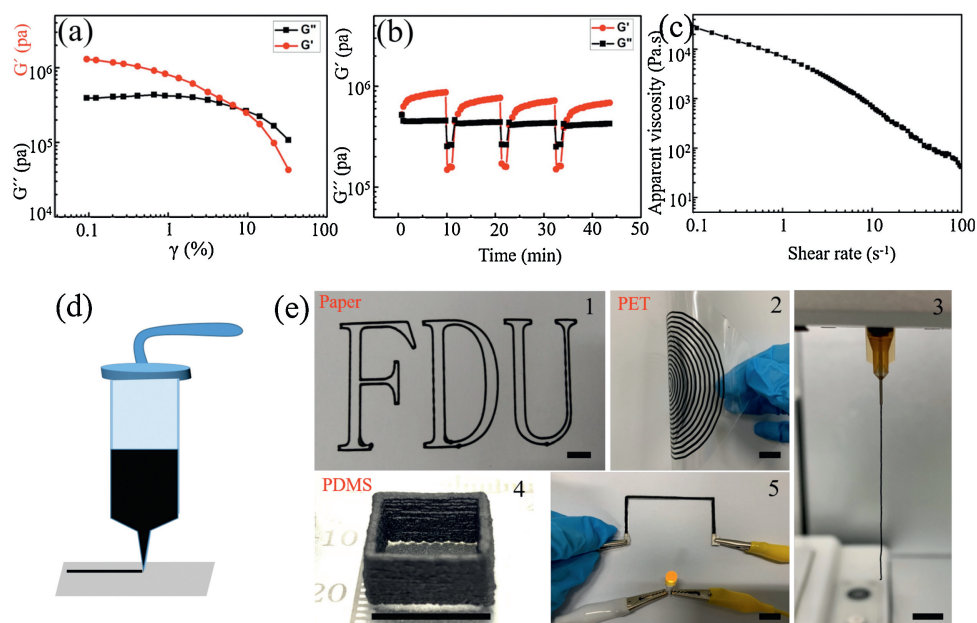


Fig. 3. (a) The curve of oscillatory strain amplitude, angular frequency = 1 rad/s. (b) G' and G'' of the composite under continuous strain sweep with alternating small oscillation force (0.1% strain) and a large one (9% strain), angular frequency = 1 rad/s. (c) The curve of viscosity against different shear rates of the 3D printing ink at room temperature. (d) Schematic illustration of the 3D printing process. (e) The photos of 3D printing patterns and circuits, the scale bars are 1 cm.

printing ink of CB/HSP composite, viscosity decreased with increasing the shear rate as depicted in Fig. 3c, showing a shear-thinning behavior. The feature, that the shear-thinning behavior under room temperature, enables the extrusion of composite at the

liquefied state which rapidly restored the solid-like state after being extruded [6]. The Schematic illustration of the 3D printing process is shown in Fig. 3d. Different patterns (width ~1 mm) were printed on paper, polyethylene terephthalate (PET) or

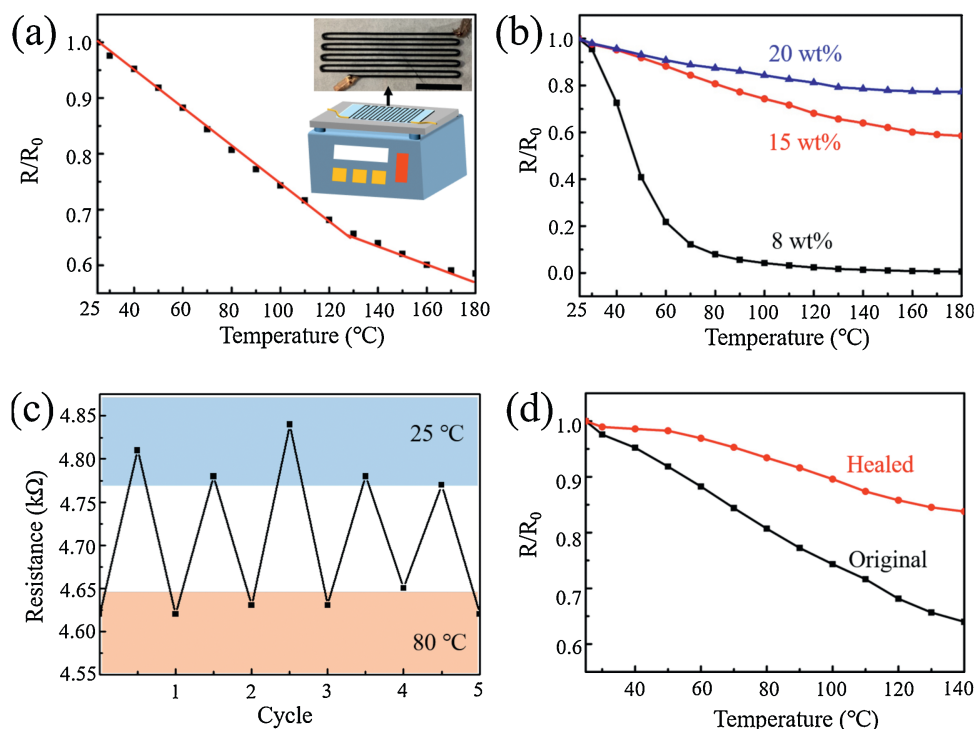


Fig. 4. (a) The curve of R/R_0 of 15 wt% composite as a function of the increase of temperature from 25 $^{\circ}\text{C}$ to 180 $^{\circ}\text{C}$. The inset is the schematic illustration of the temperature detection measurement, the scale bar is 1 cm. (b) Relative resistance change of different weight ratios of composites upon heating. (c) The resistance change of 15 wt% composite along with the repeated temperature change between 25 $^{\circ}\text{C}$ and 80 $^{\circ}\text{C}$. (d) R/R_0 change of 15 wt% composite as a function of the increased temperature that before and after self-healing.

polydimethylsiloxane (PDMS) substrates as illustrated in Fig. 3e. Owing to the strong bonding force and the flexible feature of the material, the printed circuit on PET can be bended without any deformation. The composite extruded by needles has good viscosity to form continuous lines, which can be added layer by layer to form a 3D self-supporting fence structure on PDMS (height 6.4 mm). In order to illustrate the potential application in self-healing circuit, a LED was connected to the power source by a printed CB/HSP wire (Fig. 3e), and shined at a normal voltage (3 V).

The conductivity of the 3D-printed CB/HSP circuit shows a dependence on the temperature. The thermal motion of HSP polymer segments and the electrical property of CB endow the composite with thermal sensitivity. When heating the composite, the HSP polymer wrapping on surface of CB particles moved and then the contact of CB particles increased. The resistance of the composite decreased when elevating temperature from 25 $^{\circ}\text{C}$ to 180 $^{\circ}\text{C}$ and the R/R_0 value has a linear relation with temperature (R_0 is the original resistance of the composite) as shown in Fig. 4a. Noteworthy, the sensitivity at 25 ~ 130 $^{\circ}\text{C}$ is larger than the sensitivity at 130 ~ 180 $^{\circ}\text{C}$. It can be explained as the contact of CB particles reach a certain degree that the conductivity increased slowly at higher temperature. Moreover, the decreases of resistance were getting slower upon increasing weight ratios of CB from 8 wt% to 20 wt% (Fig. 4b). It is attributed to that the more CB content will lead to their good contact in the polymer at room temperature. The resistance of 8 wt% composite varies by about 90% from 25 $^{\circ}\text{C}$ to 70 $^{\circ}\text{C}$, larger than that of the composite of carbon nanotube and HSP (about 30%) reported previously [20]. Moreover, the 15 wt% composite has a stable resistance change between 25 $^{\circ}\text{C}$ and 80 $^{\circ}\text{C}$ for five cycles as shown in Fig. 4c, displaying the stability of thermal response. To prove our temperature detector has good self-healing property, the circuit was cut and then recovered for 5 h at room temperature. The healed circuit also had thermal sensitive response though the sensitive decreased by about 20% (Fig. 4d).

In summary, we develop a 3D-printable and room-temperature healable composite conductive polymer which can be used for sensitive temperature detection. The composite exhibits good healing capacity of conductivity and mechanical property under ambient temperature. The healing efficiency can reach to 89% of mechanical property and 71% of electricity, respectively. Besides, our composite can be 3D printable on soft substrates and be used as electrical circuits. The 3D-printable property of our composite enables the manufacture of large-area, flexible electronics at a low cost. For applications, the composite shows an excellent temperature-dependent behavior of the resistance, indicating its potential application in artificial intelligence field at a low cost.

Acknowledgments

This work was supported by National Program for Thousand Young Talents of China, the National Natural Science Foundation of China (Nos. 51773041, 21544001, 21603038), Shanghai Committee of Science and Technology in China (No. 18ZR1404900), and Fudan University.

Appendix A. Supplementary data

Supplementary material related to this article can be found, in the online version, at doi:<https://doi.org/10.1016/j.ccllet.2019.06.003>.

References

- [1] M. Nadgorny, A. Ameli, *ACS Appl. Mater. Interfaces* 10 (2018) 17489–17507.
- [2] X. Kuang, K. Chen, C.K. Dunn, et al., *Appl. Mater. Interfaces* 10 (2018) 7381–7388.
- [3] J.T. Muth, D.M. Vogt, R.L. Truby, et al., *Adv. Mater.* 26 (2014) 6307–6312.
- [4] Y. Guo, Z. Ji, Y. Zhang, X. Wang, F. Zhou, *J. Mater. Chem. A* 10 (2017) 1039.
- [5] N.C. Raut, K.A. Shamery, *J. Mater. Chem. C* 6 (2018) 1618–1641.
- [6] T. Wu, E. Graya, B. Chen, *J. Mater. Chem. C* 6 (2018) 6200–6207.
- [7] W. Wu, *Nanoscale* 9 (2017) 7342.

- [8] S. Khan, L. Lorenzelli, *Smart Mater. Struct.* 26 (2017) 083001.
- [9] D. Li, W.Y. Lai, Y.Z. Zhang, W. Huang, *Adv. Mater.* 30 (2018) 1704738.
- [10] J. Stringer, T.M. Althagathi, C.C.W. Tse, et al., *Manufacturing Rev.* 3 (2016) 12.
- [11] A. Salim, S. Lim, *Sensors* 17 (2017) 2593.
- [12] S.J. Leigh, R.J. Bradley, C.P. Pursell, D.R. Billson, D.A. Hutchins, *PLoS One* 7 (2012) 365–370.
- [13] D. Zhang, B. Chi, B. Lia, et al., *Synth. Met.* 217 (2016) 79–86.
- [14] P. Cordier, F. Tournilhac, C. Soulie-Ziakovic, L. Leibler, *Nature* 451 (2008) 977–980.
- [15] K. Heymann, J. Lehmann, D. Solomon, M. Schmidt, T. Regier, *Org. Geochem.* 42 (2011) 1055–1064.
- [16] S.H. Foulger, *J. Appl. Polym. Sci.* 72 (1999) 1573–1582.
- [17] B.C. Tee, C. Wang, R. Allen, Z. Bao, *Nat. Nanotechnol.* 7 (2012) 825–832.
- [18] W. Huang, Y. Wang, Y. Chen, et al., *Adv. Healthcare Mater.* 5 (2016) 2813–2822.
- [19] M. Nadgorny, Z. Xiao, L.A. Connal, *Mol. Syst. Des. Eng.* 2 (2017) 283–292.
- [20] H. Yang, D. Qi, Z. Liu, et al., *Adv. Mater.* 28 (2016) 9175–9181.